Icarus 257 (2015) 275–289

Contents lists available at ScienceDirect

Icarus

journal homepage: www.elsevier.com/locate/icarus

Asteroid family ages

Federica Spoto [a,c,*], Andrea Milani [a], Zoran Knežević [b]

[a] Dipartimento di Matematica, Università di Pisa, Largo Pontecorvo 5, 56127 Pisa, Italy
[b] Astronomical Observatory, Volgina 7, 11060 Belgrade 38, Serbia
[c] SpaceDyS srl, Via Mario Giuntini 63, 56023 Navacchio di Cascina, Italy

ARTICLE INFO

Article history:
Received 6 December 2014
Revised 27 April 2015
Accepted 30 April 2015
Available online 14 May 2015

Keywords:
Asteroids
Asteroids, dynamics
Impact processes

ABSTRACT

A new family classification, based on a catalog of proper elements with ∼384,000 numbered asteroids and on new methods is available. For the 45 dynamical families with >250 members identified in this classification, we present an attempt to obtain statistically significant ages: we succeeded in computing ages for 37 collisional families.

We used a rigorous method, including a least squares fit of the two sides of a V-shape plot in the proper semimajor axis, inverse diameter plane to determine the corresponding slopes, an advanced error model for the uncertainties of asteroid diameters, an iterative outlier rejection scheme and quality control. The best available Yarkovsky measurement was used to estimate a calibration of the Yarkovsky effect for each family. The results are presented separately for the families originated in fragmentation or cratering events, for the young, compact families and for the truncated, one-sided families. For all the computed ages the corresponding uncertainties are provided, and the results are discussed and compared with the literature. The ages of several families have been estimated for the first time, in other cases the accuracy has been improved. We have been quite successful in computing ages for old families, we have significant results for both young and ancient, while we have little, if any, evidence for primordial families. We found 2 cases where two separate dynamical families form together a single V-shape with compatible slopes, thus indicating a single collisional event. We have also found 3 examples of dynamical families containing multiple collisional families, plus a dubious case: for these we have obtained discordant slopes for the two sides of the V-shape, resulting in distinct ages. We have found 2 cases of families containing a conspicuous subfamily, such that it is possible to measure the slope of a distinct V-shape, thus the age of the secondary collision. We also provide data on the central gaps appearing in some families. The ages computed in this paper are obtained with a single and uniform methodology, thus the ages of different families can be compared, providing a first example of collisional chronology of the asteroid main belt.

1. Introduction

One of the main purposes for collecting large datasets on asteroid families is to constrain their ages, that is the epoch of the impact event generating a collisional family. A collisional family not always coincides with the dynamical family detected by density contrast in the proper elements space. More complicated cases occur, such as a dynamical family to be decomposed in two collisional families, or the opposite case in which a collisional family is split in two density contrast regions by some dynamical instability.

Although other methods are possible, currently the most precise method to constrain the age of a collisional family (for the ages older than ∼10 Myr) exploits non-gravitational perturbations, mostly the Yarkovsky effect (Vokrouhlický et al., 2000). These effects generate secular perturbations in the proper elements of an asteroid which are affected not just by the position in phase space, but also by the Area/Mass ratio, which is inversely proportional to the asteroid diameter *D*. Thus, the main requirements are to have a list of family members with a wide range of values in *D*, enough to detect the differential effect in the secular drift of the proper elements affecting the shape of the family, and to have a large enough membership, to obtain statistically significant results.

Recently Milani et al. (2014) have published a new family classification by using a large catalog of proper elements (with >330,000 numbered asteroids) and with a classification method

* Corresponding author at: Dipartimento di Matematica, Università di Pisa, Largo Pontecorvo 5, 56127 Pisa, Italy.
E-mail address: spoto@spacedys.com (F. Spoto).

http://dx.doi.org/10.1016/j.icarus.2015.04.041
0019-1035/

improved with respect to past methods. This method is an extension of the Hierarchical Clustering Method (HCM) (Zappalá et al., 1990), with special provisions to be more efficient in including large numbers of small objects, while escaping the phenomenon of chaining. Moreover, the new method includes a feature allowing to (almost) automatically update the classification when new asteroids are numbered and their proper elements have been computed. This has already been applied to extend the classification to a source catalog with ~384,000 proper elements, obtaining a total of ~97,400 family members (Knežević et al., 2014). In this paper we are going to use the classification of Milani et al. (2014), as updated by Knežević et al. (2014), and the data are presently available on AstDyS.[1]

This updated classification has 21 dynamical families with >1000 members and another 24 with >250 members. The goal of this paper can be simply stated as to obtain statistically significant age constraints for the majority of these 45 families. Computing the ages for all would not be a realistic goal because there are several difficulties. Some families have a very complex structure, for which it is difficult to formulate a model, even with more than one collision: these cases have required or need dedicated studies. Some families are affected by particular dynamical conditions, such as orbital resonances with the planets, which result in more complex secular perturbations: these shall be the subject of continuing work. The results for families with only a moderate number of members (such as 250–300) might have a low statistical significance.

The age estimation includes several sources of uncertainty which cannot be ignored. The first source appears in the formal accuracy in the least square fit used in our family shape estimation methods. The uncertainty depends upon the noise resulting mostly from the inaccuracy of the estimation of D from the absolute magnitude H. The second source of error occurs in the conversion of the inverse slope of the family boundaries into age, requiring a Yarkovsky calibration: this is fundamentally a relative uncertainty, and in most cases it represents the largest source of uncertainty in the inferred ages. In Section 4.1 we give an estimate of this uncertainty between 20% and 30%.

As a result of the current large relative uncertainty of the calibration, we expect that this part of the work will be soon improved, thanks to the availability of new data. Thus the main result of this paper are the inverse slopes, because these are derived by using a consistent methodology and based upon large and comparatively accurate data set. Still we believe we have done a significant progress with respect to the previous state of the art by estimating 37 collisional family ages, in many cases providing the first rigorous age estimate, and in all cases providing an estimated standard deviation. The work can continue to try and extend the estimation to the cases which we have found challenging.

Since this paper summarizes a complex data processing, with output needed to fully document our procedures but too large, we decided to include only the minimum information required to support our analysis and results. Supplementary material, including both tables and plots, is available from the web site http://hamilton.dm.unipi.it/astdys2/fam_ages/.

2. Least squares fit of the V-shape

Asteroids formed by the same collisional event take the form of a V in the (proper a–$1/D$) plane. The computation of the family ages can be performed by using this V-shape plots if the family is old enough and the Yarkovsky effect dominates the spread of proper a, as explained in Milani et al. (2014, Section 5.2). The key idea is to compute the diameter D from the absolute magnitude H, assuming a common geometric albedo p_v for all the members of the family. The common geometric albedo is the average value of the known WISE albedos (Wright et al., 2010; Mainzer et al., 2011) for the asteroids in the family. Then we use the least squares method to fit the data with two straight lines, one for the low proper a (IN side) and the other for the high proper a (OUT side), as in Milani et al. (2014), with an improved outlier rejection procedure, see Carpino et al. (2003) and Section 2.4.

2.1. Selection of the fit region

Most families are bounded on one side or on both sides by resonances. Almost all these resonances are strong enough to eject most of the family members that fell into the resonances into unstable orbits. In these cases the sides of the V are cut by vertical lines, that is by values of a, which correspond to the border of the resonance. For each family we have selected the fit region taking into account the resonances at the family boundaries. The fit of the slope has to be done for values of $1/D$ below the intersection of one of the sides of the V affected by the resonance and the resonance border value of proper a. In Table 1 we report the values for a and D, and the cause of each selection.

The *cause* of each cut in proper a is a mean motion resonance, in most cases a 2-body resonance with Jupiter, in few cases either a 2-body resonance with Mars or a 3-body resonance with Jupiter and Saturn. When no resonance with this role has been identified, we use the label FB (for Family Box) to indicate that the family ends where the HCM procedure does not anymore detect a significant density contrast (with respect to the local background). This is affected by the depletion of the proper elements catalog due to the completeness limit of the surveys: the family may actually contain many smaller asteroids beyond the box limits, but they have not been discovered yet. On the contrary when the family range in proper a is delimited by strong resonances, the family members captured in them can be transported far in proper e (and to a lesser extent in proper $\sin I$) to the point of not being recognizable as members; over longer time spans, they can be transported to planet-crossing orbits and removed from the main belt altogether.

The tables in this paper are sorted in the same way: there are four parts, dedicated to families of the types fragmentation, cratering, young, one-sided; inside each group the families are sorted by decreasing number of members. In some cases the tables have been split in four sub-tables, one for each type.

In two cases we have already defined the fit region in such a way that we can include two families in a single V-shape. This *family join* is justified later, in Section 3, by showing that the two dynamical families can be generated by a single collision. This applies to the join of 10955 with 19466 and to the join of 163 with 5206. Note that the join of two families, justified by the possibility to fit together in a single V-shape with a common age, is conceptually different from the *merge* of two families due to intersections, discussed in Milani et al. (2014) and Knežević et al. (2014); however, the practical consequences are the same, namely one family is included in another one and disappears from the list of families.

For one-sided families we are also indicating the "cause" of the missing side. E.g., for 2076 the lack of the IN side of the V-shape is due to the 7/2 resonance; on the other hand, the dynamical family 883 could be the continuation of 2076 at proper a lower than the one of the resonance. However, the V-shape which would be obtained by this join would have two very different slopes, thus it can be excluded that they are the same collisional family.

For most families the "cause" of the delimitation in proper a, in the sense above, can be clearly identified. However, some ambiguous cases remain: e.g., for family 1128 the outer boundary could be

[1] http://hamilton.dm.unipi.it/astdys/index.php?pc=5.

Table 1
Fit region: family number and name, explanation of the choice, minimum value of proper a, minimum value of the diameter selected for the inner and the outer side.

Number/name	Cause	Min proper a	Min D IN	Cause	Max proper a	Min D OUT
158 Koronis	5/2	2.82	7.69	7/3	2.96	5.00
24 Themis	11/5	3.075	25.00	2/1	3.24	16.67
847 Agnia	8/3	2.70	4.55	5/2	2.82	6.67
3395 Jitka	FB	2.76	1.33	5/2	2.82	1.33
1726 Hoffmeister	3-1-1	2.75	5.00	5/2	2.82	4.00
668 Dora	3-1-1	2.75	5.88	5/2	2.815	8.33
434 Hungaria	5/1	1.87	1.25	4/1	2.00	1.25
480 Hansa	3/1?	2.54	5.00	FB	2.71	6.67
808 Merxia	8/3	2.7	2.50	FB	2.80	2.00
3330 Gantrisch	FB?	3.13	6.67	5-2-2	3.17	6.67
10955 Harig	FB	2.67	1.43	FB	2.77	1.82
293 Brasilia	5/2	2.83	2.50	FB	2.88	2.00
569 Misa	FB	2.62	3.33	FB	2.70	3.33
15124 2000EZ_{39}	FB	2.62	2.00	FB	2.70	2.50
1128 Astrid	FB?	2.755	2.22	5/2	2.82	2.22
845 Naema	FB	2.91	2.86	7/3	2.96	5.00
4 Vesta	7/2	2.25	2.50	3/1	2.50	2.94
15 Eunomia	3/1?	2.52	5.00	8/3	2.71	5.00
20 Massalia	10/3	2.33	1.00	3/1	2.50	0.91
10 Hygiea	11/5	3.07	7.14	2/1	3.25	7.69
31 Euphrosyne	11/5	3.07	6.67	2/1	3.25	6.67
3 Juno	FB?	2.62	2.00	8/3	2.70	2.50
163 Erigone	10/3	2.33	2.50	2/1M	2.42	2.50
3815 König	FB	2.56	2.20	FB	2.585	2.20
396 Aeolia	FB	2.73	1.67	FB	2.755	2.00
606 Brangane	FB	2.57	1.67	FB	2.595	1.67
1547 Nele	FB	2.64	1.67	FB	2.648	1.67
18405 1993FY_{12}	FB	2.83	2.50	FB	2.85	2.00
170 Maria	3/1?			FB	2.665	4.00
93 Minerva	FB	2.71	4.00	5/2		
2076 Levin	7/2			FB	2.34	2.50
3827 Zdenekhorsky	8/3	2.7	2.00	1-1C		
1658 Innes	3/1?			11/4	2.645	2.00
375 Ursula	FB	3.1	12.50	2/1		

due to the 3-body resonance 3-1-1 (the three integer coefficients apply to the mean motions of Jupiter, Saturn and the asteroid, respectively); for family 3 the inner boundary could be due to 4-3-1. For family 3330 a 3-body resonance (not identified) at $a = 3.129$ could be the cause of the inner boundary.

For the one-sided family 3827 we do not know the cause of the missing OUT side, although we suspect it has something to do with (1) Ceres, given that the proper a of Ceres is very close to the upper limit of the family box.

The family of (3395) Jitka is a subfamily of the dynamical family 847. The family of (15124) 2000 EZ_{39} is a subfamily of the dynamical family 569.

With 3/1? we are indicating 2 cases (480, 15) in which the families could be delimited on the IN side by the 3/1 resonance (also 170, 1658 in which the 3/1 could be the cause of the missing IN side), but the lower bound on proper a appears too far from the Kirkwood gap. This is a problem which needs to be investigated.

2.2. Binning and fit of the slopes

Next we divide the $1/D$ axis into bins, as in Figs. 1 and 2. The partition is done in such a way that each bin contains roughly the same number of members.

The following points explain the main features of the method used to create the bins:

1. the maximum number of bins N is selected for each family, depending upon the number of members of the family;
2. the maximum value of the standard deviation of the number of members in each bin is decided depending upon the number of members of the family;

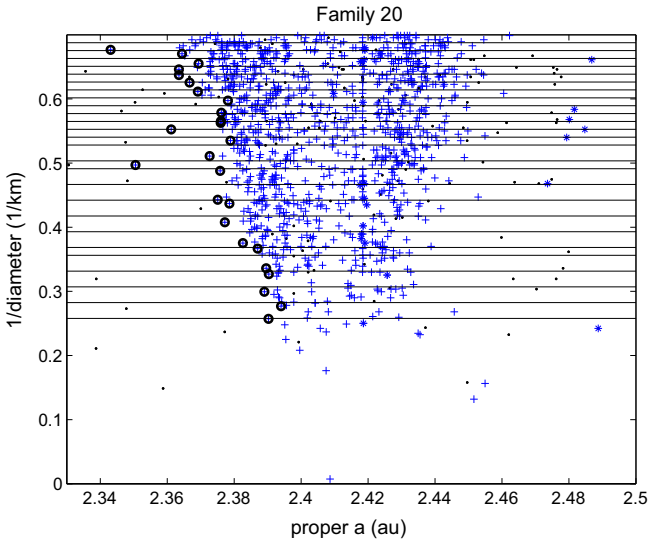

Fig. 1. Blow up of the bins for the inner side of the family of (20) Massalia. Crosses are the members of the family, points are background asteroids, stars are affected by the resonances. Circles are members of the family of (20) Massalia with the minimum value of proper a and the corresponding $1/D$ in each bin.

3. the region between 0 and the maximum value of $1/D$ is divided in N bins;
4. the difference between the number of members in two consecutive bins is computed:
   4.1 if the difference is less than the standard deviation, the bins are left as they are;

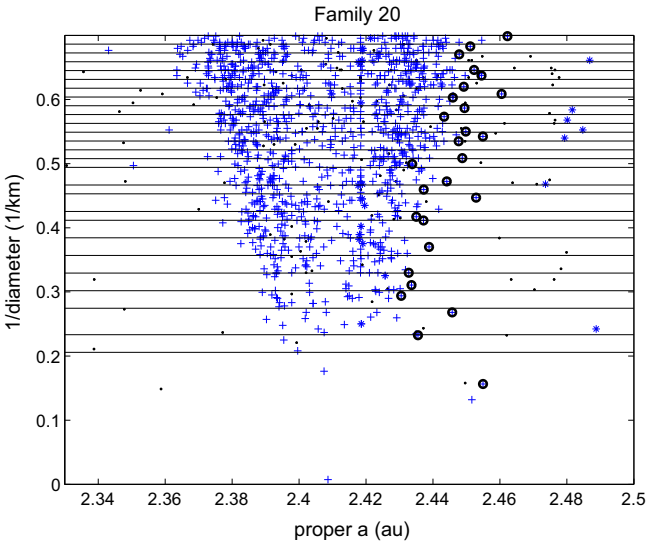

Fig. 2. Blow up of the bins for the outer side of the family of (20) Massalia. Circles are members of the family of (20) Massalia with the maximum value of proper a and the corresponding $1/D$ in each bin on the left side. Crosses, points and stars as in Fig. 1.

4.2 if the difference is greater than the standard deviation, the first bin is divided into smaller bins and then the same procedure is applied to the new bins.

This procedure is completely automatic, and it is the same both for the inner and the outer side of a V-shape. In the example of the figures, namely the family of (20) Massalia, in the IN side there are 84 bins with a mean of 19 members in each, with a STD of this number 13. In the OUT side there are 82 bins with mean 19 and STD 11.

In the case of the low a side we select the minimum value of proper a and the corresponding $1/D$ in each bin, as in Fig. 1. For the other side we select the maximum value of the proper semimajor axis and the corresponding $1/D$, as in Fig. 2. These are the data to be fit to determine the slopes of the V-shapes: thus it is important to have enough bins to properly cover the range in proper a.

2.3. Error model and weights

The least squares fit, especially if it includes an outlier rejection procedure, requires the existence of an error model for the values to be fit. Until now there are no error models for the absolute magnitude and the albedo, which are available for a large enough catalog of asteroids.

We have built a simple but realistic error model for $1/D$ computed from the absolute magnitude H (the formula is $D = 1329 \times 10^{-H/5} \times 1/\sqrt{p_v}$) by combining the effect of two terms in the error budget: the error in the absolute magnitude with STD σ_H and the one in the geometric albedo with STD σ_{p_v}. The derivatives of $1/D$ with respect to these two quantities are:

$$\frac{\partial(1/D)}{\partial H} = \frac{log(10)}{5} \times \frac{1}{D} \quad \frac{\partial(1/D)}{\partial p_v} = \left(\frac{1}{2 \times p_v}\right) \times \frac{1}{D},$$

then the combined error has STD

$$\sigma_{1/D} = \sqrt{\left(\frac{\partial(1/D)}{\partial H}\ \sigma_H\right)^2 + \left(\frac{\partial(1/D)}{\partial p_v}\ \sigma_{p_v}\right)^2}.$$

To compute this error model we need to select three values: (1) the common geometric albedo p_v for all the family members, (2) the dispersion with respect to this common albedo σ_{p_v}, and (3) the uncertainty in the absolute magnitude σ_H.

For the first two, we select all the "significant" WISE albedos, that is the values of the albedos greater than 3 times their standard deviations (with $S/N > 3$). Then we cut the tails of this distribution (see Fig. 3): p_v is the mean and σ_{p_v} is the standard deviation of the values of the albedo without the tails. For the third value σ_H we use the same for all the families and the chosen value is 0.3, see the discussion in Milani et al. (2014, Section 2.2) and Pravec et al. (2012).

The histograms such as Fig. 3 are available for all the families listed in Table 2 at the Supplementary material web site.

In Table 2 we show the albedo value of the namesake asteroid, with its uncertainty and the appropriate reference: W for WISE data (Masiero et al., 2011), I for IRAS, S for Shepard et al. (2008), and A for AKARI. In some cases albedo data are not available. The columns 5 and 6 contain the value of the albedo used for the cut of the tails, and the last two columns are the mean albedo and the standard deviation.

Two discordant results from the albedo analysis of the dynamical families are easily appreciated from Table 2. (93) Minerva and (293) Brasilia are interlopers in the dynamical families for which they are namesake, as shown by albedo data outside of the family range. Indeed, in the following of this paper we are going to speak of the family 1272 (Gefion) instead of 93, and of the family 1521 (Seinajoki) instead of 293; both are obtained by removing interlopers selected because of albedo data, and the namesake is the lowest numbered after removing the interlopers.

For many families we have proceeded in the same way, that is removing interlopers clearly indicated by an albedo discordance. The list of these interlopers for each family is in the Supplementary material.

In some cases we have joined two dynamical families for the purpose of mean albedo computation: 2076 includes 298, 163 include 5026, 10955 includes 19466,[2] Family 847 includes the subfamily 3395: the same mean albedo was used for both, although (847) has albedo 0.147 ± 0.01 and (3395) 0.313 ± 0.05, which are on the opposite side of the mean. Also 569 in Table 2 includes the subfamily 15124.

The family of (434) Hungaria is a difficult case: some WISE data exist for its family members, but they are of especially poor quality. Thus we have used for all the albedo derived from radar data (Shepard et al., 2008), and assumed a quite large dispersion (0.1).

2.4. Outlier rejection and quality control

The algorithm for differential corrections used for the computation of the slopes includes an automatic outlier rejection scheme, as in Carpino et al. (2003). Both the use of an explicit error model for the observations and the fully automatic outlier rejection procedure are implemented in the free software OrbFit[3] and are used for the orbit determination of the asteroids included in the NEODyS and AstDyS information systems.[4] Thus, although the application of these methods to the computation of family ages is new, this is a very well established procedure on which we have a lot of experience.

In practice, outlier rejection is performed in an iterative way. At each iteration, the program computes the residuals of all the observations, their expected covariance and the corresponding χ^2 value. If we can assume that the observation errors have a normal distribution, to mark an observation as an outlier we can compare the χ^2

[2] However, there is only 1 significant WISE albedo among members of family 19466.

[3] Distributed at http://adams.dm.unipi.it/orbfit/.

[4] http://newton.dm.unipi.it/neodys/ and http://hamilton.dm.unipi.it/astdys/ respectively.

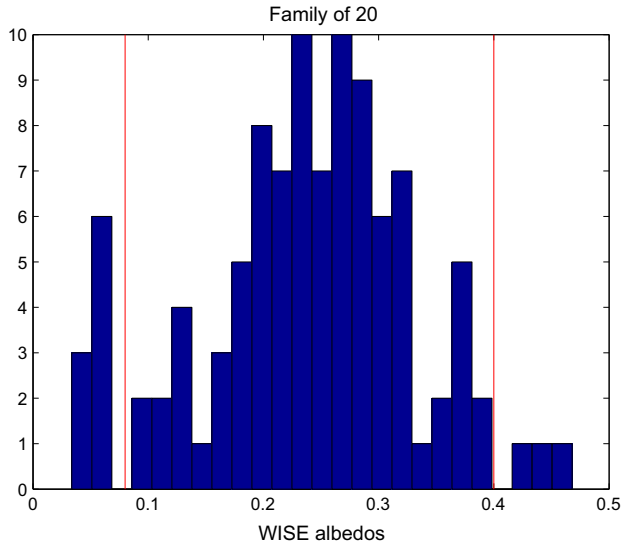

Fig. 3. Histogram of the "significant" WISE albedos for the dynamical family of (20) Massalia. The vertical lines show the values of the albedos used for the cut, leaving out values which should correspond to interlopers. In this and in many other cases the selection of the interlopers is simple: albedo <0.1 indicates C-complex asteroids and >0.4 values are likely to be affected by large errors.

value of the post-fit residual with a threshold value χ^2_{rej}: the observation is discarded if $\chi^2_i > \chi^2_{rej}$. At each iteration it is also necessary to check if a given observation, that we have previously marked as an outlier, should be recovered. Therefore, the program selects an outlier to be recovered if for the non-fitted residual $\chi^2_i < \chi^2_{rec}$. The current values for χ^2_{rej} and χ^2_{rec} are 10 and 9, respectively.

During each iteration of the linear regression we compute the residuals, the outliers, the RMS of the weighted residuals and the Kurtosis of the same weighted residuals. Our method converges if there is an iteration without additional outliers. All these data are reported in Table 1 of the Supplementary material. Besides the automatic outlier rejections, some *interlopers* have been manually removed when there was a specific evidence that they do not belong to the collisional family, e.g., based upon WISE data: also these manual rejections are detailed in the Supplementary material.

3. Results

3.1. Fragmentation families

The results of the fit for the slopes of the V-shape are described in Table 3 for the families of the fragmentation type. To define fragmentation families, we have used the (admittedly conventional) definition that the volume of the family without the largest member has to be more than 12% of the total. This computation has been done after removing the interlopers (by physical properties) and the outliers (removed in the fit), and is based on D computed with the mean albedo p_v. Comments for some of the cases are given below.

- For family 158 (Koronis) the values of the inverse slope $1/S$ on the two sides are consistent, that is the ratio is within a standard deviation from 1: this indicates that we are measuring the age of a single event. The well known subfamily of (832) Karin, with a recent age, does not affect the slopes.
- Family 24 (Themis) has the well known subfamily of (656) Beagle near the center of the V-shape, thus it does not affect the slopes. The values IN and OUT are not the same but the

Table 2
Family albedos: number and name of the family, albedo of the parent body with standard deviation and code of reference, maximum and minimum value for computing mean, mean and standard deviation of the albedo.

Number/name	Albedo value	Largest STD	Ref.	Min	Family max	Albedo mean	STD
158 Koronis	0.144	0.009	W	0.07	0.50	0.240	0.061
24 Themis	0.064	0.016	W		0.12	0.069	0.019
847 Agnia	0.147	0.012	W	0.10	0.40	0.242	0.056
1726 Hoffmeister	0.036	0.007	W		0.10	0.048	0.013
668 Dora	0.073	0.009	W		0.10	0.058	0.014
434 Hungaria	0.380		S			0.380	0.100
480 Hansa	0.249	0.024	I	0.10	0.45	0.286	0.068
808 Merxia	0.165	0.021	W	0.10	0.40	0.248	0.055
3330 Gantrisch	0.048	0.010	W			0.047	0.012
10955 Harig						0.251	0.068
293 Brasilia	0.033	0.007	W	0.10	0.27	0.174	0.042
569 Misa	0.030	0.001	I		0.10	0.058	0.016
1128 Astrid	0.046	0.018	W			0.052	0.014
845 Naema	0.072	0.019	W		0.10	0.065	0.014
4 Vesta	0.423	0.053	I	0.15	0.60	0.355	0.099
15 Eunomia	0.206	0.055	W		0.50	0.260	0.083
20 Massalia	0.210	0.030	I	0.08	0.40	0.249	0.070
10 Hygiea	0.058	0.005	W	0.02	0.15	0.073	0.022
31 Euphrosyne	0.045	0.045	W		0.10	0.061	0.015
3 Juno	0.238	0.025	I	0.10	0.40	0.253	0.055
163 Erigone	0.033	0.004	W		0.10	0.055	0.013
3815 König	0.056	0.004	W		0.15	0.051	0.014
396 Aeolia	0.139	0.025	W			0.106	0.028
606 Brangane	0.089	0.012	W			0.121	0.028
1547 Nele	0.313	0.040	A	0.15		0.355	0.064
18405 1993FY$_{12}$				0.10		0.184	0.042
170 Maria	0.160	0.007	I			0.261	0.084
93 Minerva	0.073	0.004	I	0.10	0.50	0.277	0.096
2076 Levin	0.557	0.318	W	0.10	0.40	0.202	0.070
3827 Zdenekhorsky	0.104	0.008	W		0.12	0.074	0.020
1658 Innes	0.224	0.037	W	0.10	0.43	0.264	0.064
375 Ursula	0.049	0.001	A		0.10	0.062	0.015

Table 3
Slopes of the V-shape for the fragmentation families: family number/name, number of dynamical family members, side, slope (S), inverse slope ($1/S$), standard deviation of the inverse slope, ratio OUT/IN of $1/S$, and standard deviation of the ratio.

Number/name	No. members	Side	S	$1/S$	STD $1/S$	Ratio	STD ratio
158 Koronis	6130	IN	−1.647	−0.608	0.089		
		OUT	1.755	0.570	0.069	0.94	0.18
24 Themis	4329	IN	−0.720	−1.390	0.385		
		OUT	0.477	2.096	0.326	1.51	0.48
847 Agnia	2395	IN	−2.882	−0.347	0.072		
		OUT	4.381	0.228	0.034	0.66	0.17
3395 Jitka		IN	−21.387	−0.047	0.009		
		OUT	21.214	0.047	0.008	1.01	0.26
1726 Hoffmeister	1560	IN	−5.026	−0.199	0.028		
		OUT	5.212	0.192	0.025	0.96	0.18
668 Dora	1233	IN	−3.075	−0.325	0.053		
		OUT	3.493	0.286	0.086	0.88	0.30
434 Hungaria	1187	IN	−14.855	−0.067	0.006		
		OUT	15.293	0.065	0.003	0.97	0.10
480 Hansa	960	IN	−3.710	−0.270	0.109		
		OUT	3.064	0.326	0.040	1.21	0.51
808 Merxia	924	IN	−8.400	−0.119	0.010		
		OUT	8.963	0.112	0.008	0.94	0.10
3330 Gantrisch	723	IN	−3.986	−0.251	0.061		
		OUT	3.552	0.282	0.075	1.12	0.40
10955 Harig and	517	IN	−6.515	−0.154	0.027		
19466 Darcydiegel	153	OUT	5.853	0.171	0.050	1.11	0.38
1521 Seinajoki	545	IN	−8.454	−0.118	0.023		
		OUT	23.507	0.043	0.005	0.36	0.08
569 Misa	441	IN	−5.0376	−0.199	0.151		
		OUT	6.5380	0.153	0.052	0.77	0.64
15124 $2000EZ_{39}$		IN	−14.422	−0.069	0.006		
		OUT	14.337	0.070	0.007	1.01	0.14
1128 Astrid	436	IN	−11.339	−0.088	0.006		
		OUT	11.434	0.088	0.007	0.99	0.10
845 Naema	286	IN	−11.715	−0.085	0.011		
		OUT	10.741	0.093	0.004	1.09	0.15

difference has very low statistical significance. The low accuracy of the IN slope determination is due to the fact that the 11/5 resonance cuts the V-shape too close to the center, sharply reducing the useful range in D.

- For family 847 (Agnia) we have estimated also the slopes for the subfamily 3395. 847 has discordant slope values on the two sides, but the OUT one has too few points, being affected by 3395. Thus we consider as the true value the one obtained on the IN side. 3395 has a very good fit but with many outliers, which can be explained as members of 847 but not 3395. Anyway the inverse slopes are significantly lower for 3395; since the ages are proportional to the inverse slopes, this indicates an age younger by a factor 7.42 ± 2.06 (based upon the IN values).
- Family 1726 (Hoffmeister) has an especially complicated dynamics on the IN side, due to both the nonlinear secular resonance $g + s - g_6 - s_6$ and the proximity with (1) Ceres, see the discussion in Milani et al. (2014, Section 4.1). However, the results on the two slopes are perfectly consistent: this is in agreement with what was claimed by Delisle and Laskar (2012), namely that the Yarkovsky effect prevails over the chaotic effects induced by close approaches (also by the 1-1 resonance) with Ceres, in the range of sizes which is relevant for the fit.
- For the family 480 (Hansa) the slope for the IN side has lower quality, probably due to 3/1 resonance. It is a marginal fragmentation with 14% of the total volume, excluding (480) Hansa itself.
- Family 808 (Merxia) is a fragmentation with a dominant largest member (64% in volume), thus (808) must not be included in the fit.
- For the family 3330 (Gantrisch) it has been difficult to compute a slope for the IN side, because of the irregular shape of the low a border resulting in few data to be fit.
- Family 10955 (Harig) can be joined with family 19466: in this way two one-sided families form a single V-shape: this join is confirmed by the two slopes being consistent. Thus one collisional family is obtained from two dynamical families. This merge was already suggested in Milani et al. (2014, Section 4.3.2), based on the family box overlap (by 40%).
- Family 1521 (Seinajoki) appears to have two discordant slopes: in the projection $(a, \sin I)$ a bimodality appears in the family shape. We draw from this the conclusion that there are two collisional families, the one on the IN side being older.
- The family 569 (Misa) is a marginal fragmentation (fragments account for 19% of the total volume). The ratio of the IN and OUT slopes is not significantly different from 1, mostly because of the low accuracy of the IN value. (15124) 2000 EZ_{39} appears to be the largest fragment of a fragmentation subfamily inside the family 569: the inverse slopes are significantly lower, indicating an age younger by a factor 2.19 ± 0.78 with respect to 569 (based upon the OUT values).

3.2. Cratering families

The results of the fit for the slopes of the V-shape are described in Table 4 for the families of the cratering type, defined by a volume of the family without the largest member <12% of the total. Comments for some of the cases are given below.

Table 4
Slope of the V-shape for the cratering families. Columns as in Table 3.

Number/name	No. members	Side	S	$1/S$	STD $1/S$	Ratio	STD ratio
4 Vesta	8620	IN	−2.983	−0.335	0.040		
		OUT	1.504	0.665	0.187	1.98	0.61
15 Eunomia	7476	IN	−1.398	−0.715	0.057		
		OUT	2.464	0.406	0.020	0.57	0.05
20 Massalia	5510	IN	−15.062	−0.066	0.003		
		OUT	14.162	0.071	0.006	1.06	0.10
10 Hygiea	2615	IN	−1.327	−0.754	0.079		
		OUT	1.329	0.752	0.101	1.00	0.17
31 Euphrosyne	1137	IN	−1.338	−0.747	0.096		
		OUT	1.507	0.663	0.081	0.89	0.16
3 Juno	960	IN	−5.261	−0.190	0.038		
		OUT	7.931	0.126	0.049	0.66	0.29
163 Erigone and	429	IN	−7.045	−0.142	0.035		
5026 Martes	380	OUT	6.553	0.153	0.013	1.08	0.28

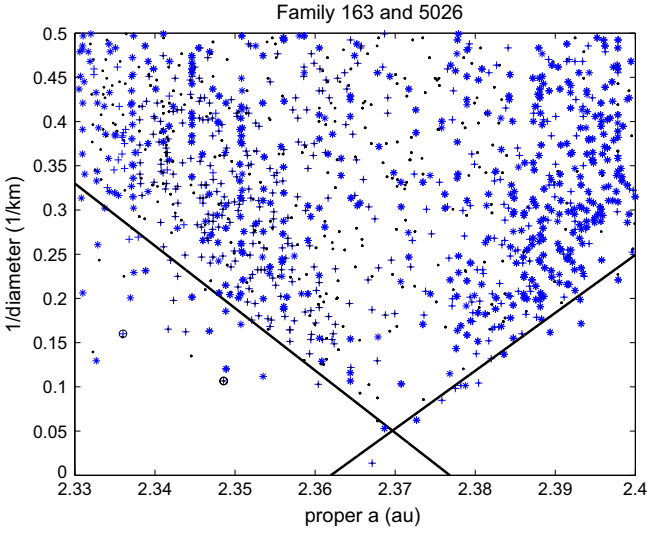

Fig. 4. V-shape fit for the join of families of (163) Erigone and (5026) Martes. The IN slope is fit to members of 163, the OUT slope to members of 5026, but the two values are consistent. The central depleted region explains why the two families have no intersection: they are *joined* but not *merged*.

- Family 4 (Vesta) has two discordant slopes on the IN and OUT sides. As already suggested in Milani et al. (2014, Section 7.2), this should be interpreted as the effect of two distinct collisional families, with significantly different ages. The estimated ratio of the slopes provides a significant estimate of the ratio of the ages, because the Yarkovsky calibration is common to the two subfamilies, corresponding to two craters on Vesta.
- Family 15 (Eunomia) has a subfamily which determines the OUT slope, the ratio of the slopes gives a good estimate of the ratio of the ages, because of the common calibration. The interpretation as two collisional families, proposed in Milani et al. (2014, Section 7.4), is thus confirmed.
- Family 10 (Hygiea) has a shape (especially in the proper (a, e) projection) from which we could suspect two collisional events, but the IN and OUT slopes not just consistent but very close suggest a single collision.
- For family 3 (Juno) the IN and OUT slopes are discordant, but due to the low relative accuracy of the slopes the difference is marginally significant. The number density as a function of proper a is asymmetric, more dense on the OUT side.
- Family 163 (Erigone) can be joined with 5026 (Martes), with (163) as parent body for both (marginally within the cratering definition, fragments forming 11% of the total volume). This is confirmed by similar albedo (dark in a region dominated by brighter asteroids) and by very consistent slopes of the IN side (formed by family 163) and of the OUT side (formed by 5026), see Fig. 4. There is a very prominent gap in the center, which explains why we have found no intersections; it should be due to the YORP effect; see Section 5.2. Again one collisional family is obtained from two dynamical families.

3.3. Young families

We define as *young families* those with an estimated age of <100 Myr; thus the inverse slopes are much lower than those of the previous tables. These can be both fragmentations and craterings. The results of the fit are described in Table 5.

These families have a comparatively low number of members, but because they also have a small range of proper a values a significant slope fit is possible. In particular we have introduced the three last families in the table with <250 members.

Few comments: families 396 (Aeolia) and 606 (Brangane) are craterings, all the others are fragmentations. The family 1547 (Nele) is a marginal fragmentation, with 19% of volume outside (1547); it is known to be very young (Nesvorný et al., 2003), it has been included to test the applicability of the V-shape method to recent families (see Section 4.2.3).

3.4. One side

The one-sided families are those for which we cannot identify one of the two sides of the V-shape. The results of the fit are described in Table 6.

The families of this type can be due to fragmentations and craterings: in most cases there is no dominant largest fragment, and they might have had parent bodies disappeared in the resonance which also wiped out one of the sides, thus we do not really know.

- The family 170 (Maria) has a possible subfamily for low proper a (no effect on the OUT slope). There is no dominant largest fragment, thus it could be either a fragmentation or a cratering, in the latter case with parent body removed by the 3/1 resonance.
- For the family 1272 (Gefion) there is no dominant largest fragment, thus the same argument applies, with possible parent body removal by the 5/2 resonance.

Table 5
Slope of the V-shape for the young families. Columns as in Table 3.

Number/name	No. members	Side	S	$1/S$	STD $1/S$	Ratio	STD ratio
3815 König	340	IN	−31.892	−0.031	0.004		
		OUT	31.364	0.032	0.004	1.02	0.17
396 Aeolia	306	IN	−32.358	−0.031	0.005		
		OUT	35.556	0.028	0.005	0.91	0.22
606 Brangane	192	IN	−54.027	−0.019	0.002		
		OUT	60.374	0.017	0.003	0.89	0.17
1547 Nele	152	IN	−201.336	−0.005	0.0008		
		OUT	187.826	0.005	0.002	1.07	0.44
18405 $1993FY_{12}$	102	IN	−34.189	−0.029	0.01		
		OUT	34.456	0.029	0.005	0.99	0.36

Table 6
Slopes of the V-shape for the one-sided families: family number/name, number of dynamical family members, side, slope (S), inverse slope ($1/S$), standard deviation of the inverse slope.

Number/name	No. members	side	S	$1/S$	STD $1/S$
170 Maria	1431	OUT	1.487	0.672	0.059
1272 Gefion	1341	IN	−2.594	−0.386	0.094
2076 Levin	1237	OUT	7.080	0.141	0.023
3827 Zdenekhorsky	794	IN	−10.871	−0.092	0.009
1658 Innes	606	OUT	6.006	0.167	0.011
375 Ursula	335	IN	−0.516	−1.938	0.426

- For family 2076 (Levin) the possibility of merging with families 298 (Baptistina) and 883 has been discussed in Milani et al. (2014, Section 4.1). Joining Baptistina does not change the slopes; joining 883 would result in a two-sided V-shape, with a gap due to the 7/2 resonance in between; however, the two slopes would be very different. All three dynamical families (for which we already have some intersections) could be considered as a single complex dynamical family, but still they would belong to different collisional families with different ages. The slope (thus the age) we have computed belongs to the event generating only the 2076 family. There are not enough significant physical data on the members of these families,[5] not even on the comparatively large (298), to help us in disentangling this complex case.
- Family 1658 (Innes) is the largest fragment but it is not dominant in size, thus we cannot distinguish between fragmentation and cratering with parent body removed by the 3/1 resonance.
- (375) Ursula is an outlier in the fit for the IN slope of 375. This can have two interpretations. Either (375) is the largest fragment of a marginal fragmentation (fragments are 23% of total volume), in which case it is correct not to include it in the slope fit, or (375) is an interloper and the family could have had a parent body later disappeared in the 2/1 resonance. Unfortunately, it is difficult to use albedo data to help on this, because there is no albedo contrast with the background.

4. Age estimation

4.1. Yarkovsky calibrations

The method we use to convert the inverse slopes from the V-shape fit into family ages has been established in Milani et al. (2014, Section 5.2), and consists in finding a *Yarkovsky calibration*, which is the value of the Yarkovsky driven secular drift da/dt for an hypothetical family member of size $D = 1$ km and with spin axis obliquity (with respect to the normal to the orbital plane) 0° for the OUT side and 180° for the IN side. Since the inverse slope is the change $\Delta(a)$ accumulated over the family age by a family member with unit $1/D$, the age is just $\Delta(t) = \Delta(a)/(da/dt)$.

The question is how to produce the Yarkovsky calibration. As discussed in Milani et al. (2014, Section 5.2.6), this can be done in different ways depending upon which data are available. Unfortunately for main belt asteroids there are too few data to compute any calibration: indeed, a measured da/dt is available for not even one main belt object. The solution we have used was to extrapolate from the data available for Near Earth Asteroids. The best estimate available for da/dt is the one of asteroid (101955) Bennu, with a $S/N \simeq 200$ (Chesley et al., 2014). By suitable modeling of the Yarkovsky effect, by using the available thermal properties measurements, the density of Bennu has been estimated as $\rho_{Bennu} = 1.26 \pm 0.07$ g/cm^3. Bennu is a B-type asteroid, thus it is possible to compute its porosity by comparison with the very large asteroid (704) Interamnia which is of the same taxonomic type and has a reasonably well determined bulk density (Carry, 2012).

In Table 7 we list the data on benchmark large asteroids with known taxonomy and density. For the other taxonomic classes we estimate the density at $D = 1$ km by assuming the same porosity of Bennu and the same composition as the largest asteroid of the same taxonomic class. Thus in the table the density at $D = 1$ km for B class is the one of Bennu from Chesley et al. (2014), the ones for the other classes are obtained by scaling.

Once an estimate of the density ρ is available, the scaling formula can be written as:

$$\frac{da}{dt} = \left.\frac{da}{dt}\right|_{Bennu} \frac{\sqrt{a}_{(Bennu)}(1-e^2_{Bennu})}{\sqrt{a}(1-e^2)} \frac{D_{Bennu}}{D} \frac{\rho_{Bennu}}{\rho} \frac{\cos(\phi)}{\cos(\phi_{Bennu})} \frac{1-A}{1-A_{Bennu}}$$

where $D = 1$ km used in this scaling formula is not the diameter of an actual asteroid, but it is the reference value corresponding to the inverse slope; we also assume $\cos(\phi) = \pm 1$, depending upon the IN/OUT side.

The additional terms which we would like to have in the scaling formula are thermal properties, such as thermal inertia or thermal conductivity: the problem is that these data are not available. To replace the missing thermal parameters with another scaling law would not give a reliable result, also because of the strong nonlinearity of the Yarkovsky effect as a function of the conductivity, as shown in Vokrouhlický et al. (2000, Fig. 1).

We are not claiming this is the best possible calibration for each family. However, for generating a homogeneous set of family ages, we have to use a uniform method for all. To improve the calibration (thus to decrease the uncertainty of the age estimate) for a specific family is certainly possible, but requires a dedicated effort in both acquiring observational data and modeling. E.g., the Yarkovsky effect could be measured from the orbit determination for a family member (going to be possible with data from the

[5] E.g., (2076) has WISE data $p_v = 0.56 \pm 0.32$.

astrometric mission GAIA), thermal properties could be directly measured with powerful infrared telescopes, densities can be derived for binaries by using radar observations, for the cases with missing taxonomy it could be obtained by spectrometry/infrared/polarimetry. A good example is given by a very recent event: on January 26, 2015 the asteroid (357439) 2004 BL_{86} had a very close approach to the Earth, with minimum distance 0.008 au. Thus it has been possible by radar to confirm that it has a satellite, and to measure its diameter; infrared observations allowed to assign this asteroid to the taxonomic class V. When all the data are analyzed and published, we expect to have for (357439) an estimated density (from the satellite orbit and the volume, both from the radar data). This could provide a Yarkovsky calibration, specifically for the Vesta families, significantly better than the one of this paper.

This implies that the main results of this paper are the inverse slopes, from which the ages can continue to be improved as better calibration data become available.

Table 7
Benchmark asteroids for the density of a taxonomic type: number/name, taxonomic type, densities as in Carry (2012) with their uncertainties, densities at 1 km.

Number/name	Tax type	ρ	STD (ρ)	ρ (1 km)
4 Vesta	V	3.58	0.15	2.30
10 Hygiea	C	2.19	0.42	1.41
15 Eunomia	S	3.54	0.20	2.275
216 Kleopatra	Xe	4.27	0.15	2.75
704 Interamnia	B	1.96	0.28	1.26

In Table 8 we are summarizing the data used to compute the calibration. The eccentricity used in the calibration is selected, separately for the IN and OUT side, as an approximate average of the values of proper eccentricity for the family members with proper semimajor axis close to the limit. It is clear that the extrapolation from Near Earth to main belt asteroids introduces a model uncertainty, which is not the same in all cases. If a family has a well determined taxonomic type, which corresponds to one of the benchmark asteroids, our computation of the calibration is based on actual data and we assign to this case a comparatively low relative calibration STD of 0.2; these cases are labeled with the code "m". We have also estimated the Bond albedo A, which is used in the scaling, from the mean geometric albedo p_v by WISE. For subfamilies 3395 (inside 847) and 15124 (inside 569) we have assumed the same taxonomy as the larger family.

Then there are cases in which the taxonomic class is similar, but not identical to the one of the benchmark. (1726) is of type Cb, (668) of type Ch in the SMASSII classification, both assimilated to a generic C type; (808) is Sq, (1272) is SI in SMASSII, (1658) is AS in the Tholen classification, all assimilated to a generic S type. These are labeled with the code "a" and we have assigned a relative STD of 0.25.

Finally we have 7 cases in which we do not have taxonomic data at all, but just used the mean WISE albedo of Table 2 to guess a simplistic classification into a C vs. S complex. These are labeled "g" and have a relative STD of 0.3. Thus these are the worst cases from the point of view of age uncertainty, but they are the easiest to improve by observations.

Table 8
Data for the Yarkovsky calibration: family number and name, proper semimajor axis a and eccentricity e for the inner and the outer side, 1-A, density value ρ at 1 km, taxonomic type, a flag with values m (measured) a (assumed) g (guessed), and the relative standard deviation of the calibration.

Number/name	Proper a IN	Proper e IN	Proper a OUT	Proper e OUT	1-A	ρ (1 km)	Tax. type	Flag m	Rel. STD
158 Koronis	2.83	0.044	2.93	0.06	0.92	2.275	S	m	0.20
24 Themis	3.085	0.14	3.23	0.135	0.98	1.41	C	m	0.20
847 Agnia	2.73	0.07	2.81	0.07	0.92	2.275	S	m	0.20
3395 Jitka	2.762	0.07	2.81	0.07	0.92	2.275	S	m	0.20
1726 Hoffmeister	2.76	0.05	2.8	0.046	0.98	1.41	C	a	0.25
668 Dora	2.76	0.19	2.8	0.197	0.98	1.41	C	a	0.25
434 Hungaria	1.92	0.07	1.97	0.07	0.87	2.75	Xe	g	0.30
480 Hansa	2.55	0.04	2.69	0.035	0.91	2.45	S	m	0.20
808 Merxia	2.71	0.135	2.78	0.13	0.92	2.45	S	m	0.20
3330 Gantrisch	3.13	0.195	3.16	0.198	0.98	1.41	C	g	0.30
10955 Harig and	2.67	0.016			0.92	2.275	S	g	0.30
19466 Darcydiegel			2.77	0.009	0.92	2.275	S	g	0.30
1521 Seinajoki	2.84	0.12	2.866	0.123	0.94	2.275	S	g	0.30
569 Misa	2.63	0.177	2.69	0.175	0.98	1.41	C	a	0.25
15124 $2000EZ_{39}$	2.64	0.178	2.67	0.177	0.98	1.41	C	a	0.25
1128 Astrid	2.767	0.048	2.81	0.048	0.98	1.41	C	m	0.20
845 Naema	2.92	0.035	2.95	0.036	0.98	1.41	C	m	0.20
4 Vesta	2.27	0.09	2.44	0.11	0.88	2.3	V	m	0.20
15 Eunomia	2.53	0.15	2.69	0.15	0.92	2.275	S	m	0.20
20 Massalia	2.35	0.162	2.46	0.162	0.92	2.275	S	m	0.20
10 Hygiea	3.08	0.13	3.24	0.11	0.98	1.41	C	m	0.20
31 Euphrosyne	3.11	0.17	3.2	0.21	0.98	1.41	C	m	0.20
3 Juno	2.62	0.235	2.69	0.235	0.92	2.275	S	m	0.20
163 Erigone and	2.34	0.208			0.98	1.41	C	m	0.20
5026 Martes			2.37	0.207	0.98	1.41	C	m	0.20
3815 König	2.57	0.13	2.58	0.14	0.98	1.41	C	a	0.25
396 Aeolia	2.735	0.168	2.743	0.167	0.97	2.75	Xe	a	0.25
606 Brangane	2.579	0.18	2.59	0.18	0.96	2.275	S	m	0.20
1547 Nele	2.64	0.269	2.646	0.269	0.88	2.275	S	g	0.30
18405 $1993FY_{12}$	2.83	0.106	2.86	0.106	0.94	2.275	S	g	0.30
170 Maria			2.65	0.08	0.91	2.275	S	m	0.20
1272 Gefion	2.74	0.13			0.92	2.275	S	a	0.25
2076 Levin			2.31	0.14	0.93	2.275	S	g	0.30
3827 Zdenekhorsky	2.71	0.087			0.98	1.41	C	m	0.20
1658 Innes			2.61	0.17	0.91	2.275	S	g	0.30
375 Ursula	3.13	0.08			0.98	1.41	C	m	0.20

4.2. Ages and their uncertainties

The results on the ages are presented in Tables 9–12, each containing the Yarkovsky calibration, computed with the data of Table 8, the estimated age and three measures of the age uncertainty.

The first uncertainty is the standard deviation of the inverse slope, as output from the least square fit, divided by the calibration. The second is the age uncertainty due to the calibration uncertainty from the last column of Table 8: this relative uncertainty is multiplied by the estimated age. The third is the standard deviation of the age, obtained by combining quadratically the STD from the fit with the STD from the calibration.

The first uncertainty is useful when comparing ages which can use the same calibration, such as ages from the IN and from the OUT side (as shown in the last two columns of Tables 3–6); this

Table 9
Age estimation for the fragmentation families: family number and name, da/dt, age estimation, uncertainty of the age due to the fit, uncertainty of the age due to the calibration, and total uncertainty of the age estimation.

Number/name	Side (IN/OUT)	da/dt (10^{-10} au/d)	Age (Myr)	STD(fit) (Myr)	STD(cal) (Myr)	STD(age) (Myr)
158 Koronis	IN	−3.40	1792	262	358	444
	OUT	3.34	1708	206	342	399
24 Themis	IN	−5.68	2447	678	489	836
	OUT	5.54	3782	588	756	958
847 Agnia	IN	−3.46	1003	207	201	288
	OUT	3.41	669	100	134	167
3395 Jitka	IN	−3.44	136	25	27	37
	OUT	3.41	138	24	28	37
1726 Hoffmeister	IN	−5.90	337	47	84	96
	OUT	5.86	328	42	82	92
668 Dora	IN	−6.11	532	87	133	159
	OUT	6.08	471	141	118	184
434 Hungaria	IN	−3.23	208	19	62	65
	OUT	3.18	205	8	62	62
480 Hansa	IN	−3.53	763	310	153	346
	OUT	3.44	950	117	190	223
808 Merxia	IN	−3.52	338	28	68	73
	OUT	3.47	321	24	64	69
3330 Gantrisch	IN	−5.75	436	105	131	168
	OUT	5.73	492	131	148	197
10955 Harig and	IN	−3.48	441	78	132	154
19466 Darcydiegel	OUT	3.42	500	146	150	209
1521 Seinajoki	IN	−3.50	338	66	101	121
	OUT	3.49	122	15	37	40
569 Misa	IN	−6.23	319	242	80	255
	OUT	6.15	249	85	62	105
15124 $2000EZ_{39}$	IN	−6.22	111	10	28	29
	OUT	6.18	113	11	28	30
1128 Astrid	IN	−5.89	150	11	30	32
	OUT	5.85	150	11	30	32
845 Naema	IN	−5.73	149	19	30	35
	OUT	5.70	163	8	33	34

Table 10
Age estimation for the cratering families. Columns as in Table 9.

Number/name	Side (IN/OUT)	da/dt (10^{-10} au/d)	Age (Myr)	STD(fit) (Myr)	STD(cal) (Myr)	STD(age) (Myr)
4 Vesta	IN	−3.60	930	112	186	217
	OUT	3.49	1906	537	381	659
15 Eunomia	IN	−3.66	1955	155	391	421
	OUT	3.55	1144	57	229	236
20 Massalia	IN	−3.81	174	7	35	35
	OUT	3.73	189	16	38	41
10 Hygiea	IN	−5.67	1330	139	266	300
	OUT	5.50	1368	183	274	329
31 Euphrosyne	IN	−5.71	1309	169	262	312
	OUT	5.72	1160	142	232	272
3 Juno	IN	−3.46	550	110	110	156
	OUT	3.41	370	143	74	161
163 Erigone and	IN	−6.68	212	53	42	68
5026 Martes	OUT	6.64	230	46	19	50

Table 11
Age estimation for the young families. Columns as in Table 9.

Number/name	Side (IN/OUT)	da/dt (10^{-10} au/d)	Age (Myr)	STD(fit) (Myr)	STD(cal) (Myr)	STD(age) (Myr)
3815 König	IN	−6.21	51	6	13	14
	OUT	6.21	51	6	13	14
396 Aeolia	IN	−3.09	100	18	25	31
	OUT	3.08	91	15	23	27
606 Brangane	IN	−3.82	48	4	10	10
	OUT	3.81	44	7	9	11
1547 Nele	IN	−3.61	14	2	4	5
	OUT	3.61	15	5	5	7
18405 $1993FY_{12}$	IN	−3.50	83	28	25	37
	OUT	3.48	83	13	25	28

Table 12
Age estimation for the one-sided families. Columns as in Table 9.

Number/name	Side (IN/OUT)	da/dt (10^{-10} au/d)	Age (Myr)	STD(fit) (Myr)	STD(cal) (Myr)	STD(age) (Myr)
170 Maria	OUT	3.48	1932	169	386	422
1272 Gefion	IN	−3.50	1103	270	276	386
2076 Levin	OUT	3.86	366	59	110	125
3827 Zdenekhorsky	IN	−5.99	154	14	31	34
1658 Innes	OUT	3.59	464	31	139	143
375 Ursula	IN	−5.56	3483	765	697	1035

can be applied also to the cases of subfamilies. The third uncertainty is applicable whenever the absolute age has to be used, as in the case in which the ages of two different families, with independent calibration errors, are to be compared.

Among the figures, not included in this paper but available in the Supplementary material site, there are all the V-shape plots, which can be useful to better appreciate the robustness of our conclusions.

In this section we also comment on ages for the same families found in the scientific literature, with the warning that for some families there are multiple estimates, including discordant ones, in some cases published by the same authors at different times. Thus we think it is important to have a source of ages computed with a uniform and well documented procedure, such as this paper. Compilations of ages, such as Nesvorný et al. (2005) and Brož et al. (2013), are useful for consultation, but have the limitation of mixing results obtained with very different methods, sometimes even with methods not specified. We use the terminology *consistent* when one nominal value is within the STD of the other, *compatible* when difference of nominal values is less than the sum of the two STD, *discordant* otherwise.

4.2.1. Ages of fragmentation families

The ages results are in Table 9; comments on specific families follows:

158 (Koronis): the present estimate increases somewhat the result we reported in Milani et al. (2014, Table 10) of 1500 Myr for the OUT side (the result for the IN side was considered of lower quality), but within the fit uncertainty. Now the results from the two sides are not just consistent but very close, and the fit uncertainty has slightly improved (in Table 10 of the previous paper the calibration uncertainty was not included). The earliest estimates in the literature were just upper bounds of $\leqslant$2 Gyr (Marzari et al., 1995; Chapman et al., 1996), followed by (Greenberg et al., 1996; Farinella et al., 1996) who give $\sim$2 Gyr; Brož et al. (2013) give 2.5 ± 1 Gyr, which is consistent with our results: our improvement in accuracy is significant.

24 (Themis): the two sides give different values which are not discordant, but are affected by large uncertainties. This is one of the oldest families, for which there are few ages estimates in the literature: Marzari et al. (1995) give 2 Gyr.

847 (Agnia): the new result is consistent with the one of Milani et al. (2014, Table 10) for the IN side; the OUT side is anyway degraded by the presence of the 3395 subfamily.

3395 (Jitka): the results are almost the same as in Milani et al. (2014, Table 10). In the literature there are estimates for the age of Agnia, in Vokrouhlický et al. (2006a) of 100^{+30}_{-20} Myr, but from their Fig. 1 it is clear that their Agnia family is restricted to our Jitka subfamily, apart from the addition of (847) Agnia itself. Also in Brož et al. (2013) there is an estimate for 847 of 200 ± 100 Myr. Thus our results on the age are consistent with all the others, even if we disagree on the name of the family.

1726 (Hoffmeister): our result is consistent with the one in Nesvorný et al. (2005) and Brož et al. (2013), giving 300 ± 200 Myr, but with significantly lower uncertainty. The fact that the perturbations from (1) Ceres do not appear to disturb an evolution model based on the Yarkovsky secular drift is a confirmation of the statement by Delisle and Laskar (2012): chaotic perturbations from other asteroids are less effective in shifting the semimajor axis than Yarkovsky for the objects with $D < 40$ km.

668 (Dora): the OUT result is somewhat degraded by the 5/2 resonance, thus the IN is better, but anyway they are consistent. Brož et al. (2013) give 500 ± 200 Myr, in good agreement, notwithstanding the much lower distance cutoff used to define the family (60 m/s vs. our 90).

434 (Hungaria): with a similar but less rigorous method, Milani et al. (2010) find 274 Myr, which is higher but practically consistent with the current result. Warner et al. (2009) give $\sim$500 Myr, but with a low accuracy method.

480 (Hansa): in the literature we find only Carruba (2010) and Brož et al. (2013) giving as upper bound <1.6 Gyr. Our result is much more informative, especially from the OUT side.

808 (Merxia): our results are consistent with both (Brož et al., 2013) 300 ± 200 Myr, and (Nesvorný et al., 2005) 500 ± 200, but significantly more precise.

3330 (Gantrisch): we have found nothing in the literature on the age of this family, thus the result is useful even if the relative accuracy is poor.

10955 (Harig), including 19466: a well determined slope, consistent between the two sides, thus confirming the join. The absolute age is of limited accuracy because of the lack of physical observations. No previous estimates found in the literature.

1521 (Seinajoki) has two significantly different ages, younger for the OUT side. This is an additional case of a dynamical family containing two collisional families. Nesvorný et al. (2005) gives 50 ± 40 Myr, which is compatible with our estimate for the OUT side.

1128 (Astrid) has a perfect agreement on the two sides, which appears as a coincidence since the uncertainty is much higher. Nesvorný et al. (2005) give 100 ± 50 which is consistent, our estimate being more precise.

845 (Naema) has a good agreement on the two sides. Nesvorný et al. (2005) give 100 ± 50 which is compatible, our estimate being more precise.

4.2.2. Ages of cratering families

The ages results are in Table 10; comments on each family follow.

4 (Vesta): the idea that Vesta might have suffered two large impacts generating two families Milani et al. (2014, Section 7.3) is quite natural given that cratering does not decrease the collisional cross section, and has been proposed long ago (Farinella et al., 1996). The new error model and outlier rejection procedure have reduced the fit uncertainty, especially for the OUT side, thus the ratio of values on the two sides has increased its level of significance (see Table 4). The good agreement of the age from the IN side with the cratering age of the Rheasilvia basin, 1 Gyr according to Marchi et al. (2012) is very interesting. Only a rough lower bound age of $\sim$2 Gyr is available for the Veneneia basin because of the disruption due to the impact forming Rheasilvia (O'Brien et al., 2014). Thus our age estimate from the OUT side is an independent constraint to the age of Veneneia.

15 (Eunomia): in Milani et al. (2014, Table 10) the difference in the slopes for the two sides was much smaller and the fit uncertainty for the OUT side much larger, thus the existence of two separate ages was proposed as possible. The improved results provide a ratio very significantly different from 1, thus the existence of two collisional families inside the single dynamical family 15 is now supported by high S/N evidence. Nesvorný et al. (2005) give 2.5 ± 0.5 Gyr as age for the entire family, which is compatible with our IN side age.

20 (Massalia): our new results are very similar to the ones of our previous paper as well as consistent with Vokrouhlický et al. (2006b), giving as most likely an age between 150 and 200 Myr. On the contrary Nesvorný et al. (2003) give 300 ± 100 which is marginally compatible.

10 (Hygiea): the interesting point is that this dynamical family appears to have a single age, a non-trivial result since the family has a bimodal shape in the proper (a, e) projection, and (10) has almost the same impact cross section as (4) Vesta. In the literature we found only Nesvorný et al. (2005) giving a consistent, but low accuracy, 2 ± 1 Gyr.

31 (Euphrosine): This high proper $\sin I$ family is crossed by many resonances, nevertheless the age can be estimated. In the literature, we found only the upper bound <1.5 Gyr in Brož et al. (2013).

3 (Juno): the two ages IN and OUT are not consistent but only compatible; more data are needed to assess the possibility of multiple collisions. In the literature we found only an upper bound <700 Myr in Brož et al. (2013).

163 (Erigone): another very good example of join of two dynamical families, 163 and 5026, into a collisional family with all the properties expected, including age estimates consistent (within half of STD) and a lower number density in a central strip. Vokrouhlický et al. (2006b) give an age 280 ± 112 Myr, which is higher but consistent; Bottke et al. (2015) by a different method give an age 170^{+25}_{-30}, which is lower but consistent with the IN side. From the figures we can deduce that in both papers their family 163 also includes our 5026.

4.2.3. Ages of young families

The ages results are in Table 11. We are interested in finding a lower limit for the ages we can compute with the V-shape method. For most of these asteroids there are in the literature only either upper bounds or low relative accuracy estimates of the ages (Brož et al., 2013). In order of estimated age:

1547 (Nele): for this family Brož et al. (2013) give an age <40 Myr; Nesvorný et al. (2003) give a constraint $\leqslant$5 Myr on the age of the Iannini cluster, which he identified as composed of 18 members not including (1547). Our estimate (for a family with $152 - 3 = 149$ members, including (4652) Iannini) is higher, but such a young age could be too much affected by the effect of the initial velocity field, which is apparent in the anti-correlation between proper a, e. From this example we conclude that probably 15 Myr is too young to be an accurate estimate by the V-shape method; this family should be dated by a method using also the evolution of the angles ϖ, Ω.

3815 (König): we have a precise estimate, in the literature we have found only an upper bound <100 Myr (Brož et al., 2013).

606 (Brangane): also a precise estimate, in good agreement with 50 ± 40 in Brož et al. (2013). We do not have a ground truth to assess the systematic error due to contamination from the initial velocity spread, which for these ages may not be negligible.[6]

396 (Aeolia): also a precise estimate, consistent with the upper bound <100 Myr in Brož et al. (2013). 18405 ($1993FY_{12}$): Brož et al. (2013) give an age <200 Myr. Our estimate is precise and not just consistent, but the same on the two sides. For this range of ages around 100 Myr the initial velocity field should not matter.

From these examples we can conclude that the V-shape method is applicable to *young* families with ages below 100 Myr, but there is some lower age limit t_{min} such that younger ages are inaccurately estimated from the V-shape. The cases we have analyzed suggest that $t_{min} > 15$ Myr, but we do not have enough information to set an upper bound for t_{min}.

4.2.4. Ages of one-sided families

The ages results are in Table 12; these ages are based upon the assumption that only one side of the family V-shape is preserved. Of course if this was not the case, ages younger by factor roughly 2 would be obtained. For each case, comments on the justification of the one-side assumption are given below.

170 (Maria): the very strong 3/1 resonance with Jupiter makes it impossible for asteroids of the IN side of the family to have survived in the main belt, moreover the shape of the family in the $(a, 1/D)$ plane is unequivocally one sided. This is an ancient family, and our age estimate is compatible with 3 ± 1 Gyr given in Nesvorný et al. (2005), but we have significantly decreased the estimate, to the point that this cannot be a "LHB" family, as suggested by Brož et al. (2013).

1272 (Gefion): the very strong 5/2 resonance with Jupiter makes it impossible for most asteroids of the OUT side of the family to have survived in the main belt. Thus there is no OUT side in the V-shape.[7] Nesvorný et al. (2005) give an age 1.2 ± 0.4 Gyr, in

[6] A size independent velocity spread is removed by our fit method, but there may well be a $1/D$ dependency in this spread.

[7] See the figure 1272_vshapea.eps in the Supplementary material.

good agreement with ours, while Nesvorný et al. (2009, Fig. 1) show a one-sided model, giving a discordant age of 480 ± 50 Myr.

2076 (Levin): as discussed in Section 3, this could be just a component of a complex family, possibly including 298 and 883. The OUT slope, thus the age we have estimated, refers to the event generating 2076, while 298 and 883 have too few members for a reliable age. In the literature there are ages for the family of (298) Baptistina: e.g., Bottke et al. (2007) give a discordant age of 160^{+30}_{-20} Myr, but they refer to a two-sided V-shape including our 883, with an enormous number of outliers.

3827 (Zdenekhorsky): the family shape is obviously asymmetric, with much fewer members on the OUT side.[8] This prevents a statistically significant determination of the OUT slope. The family is not abruptly truncated, possibly because the effect of (1) Ceres is weaker than the one of the main resonances with Jupiter.

1658 (Innes): the shape of the family in the $(a, 1/D)$ plane is clearly one-sided. The family ends on the IN side a bit too far from the 3/1 resonance, thus the dynamics of the depletion on the IN side remains to be investigated.

375 (Ursula): the strongest 1/2 resonance with Jupiter makes it impossible for most asteroids of the OUT side of the family to have survived in the main belt. This prevents a statistically significant determination of the OUT slope. With an age estimated at $\sim 3.5 \pm 1$ Gyr, this family could be the oldest for which we have an age. Brož et al. (2013) give the upper bound <3.5 Gyr.

5. Conclusions and future work

In this paper we have computed the ages of 37 collisional families.[9] The members of these collisional families belong to 34 dynamical families, including 30 of those with >250 members. Moreover, we have computed uncertainties based on a well defined error model: the standard deviations for the ages are quite large in many cases, but still the signal to noise ratio is significantly >1.

5.1. Main results

In Fig. 5 we have placed the families on the horizontal axis with the same order used in the tables, separated in four categories.[10]

On the vertical axis (in a logarithmic scale) we have marked the estimated age with a 1 STD error bar. To avoid overcrowding of the figure, for the families with compatible ages from the IN and OUT side we have used the average (weighted with the inverse square of the STD) as the nominal with an error bar $\sigma = \sqrt{\sigma_{IN}^2 + \sigma_{OUT}^2}/2$. If the two ages are incompatible we have plotted the two estimates with the corresponding bars.[11] We have also used an informal terminology by which families are rated by their age: *primordial* with age >3.7 Gyr, *ancient* with age between 1 and 3.7 Gyr, *old* with age between 0.1 and 1 Gyr, and finally the adjective *young*, as used previously, is for ages <0.1 Gyr.

By looking at Fig. 5 it is apparent that we have been quite successful in computing ages for old families, we have significant results for both young and ancient, while we have little, if any, evidence for primordial families. This should not be rated as a surprise: already Brož et al. (2013), while specifically searching for primordial families, found a very short list of candidates, out of which 4, 10, 15, 158 and 170 we are showing to be ancient, but not primordial. From our results, only two families could be primordial, 24 and 375, although they are more likely to be just ancient. Thus we agree with the conclusion by Vokrouhlický et al. (2010) that most of the primordial families, which undoubtedly have existed, have been depleted of members to the point of not being recognized by statistically significant number density contrast: our results indicate that this conclusion applies not only to the Cybele region (beyond the 2/1 resonance) but to the entire main belt.

Fig. 5 also shows that our results allow many statistically significant absolute age comparisons between different families. Although the results should be improved, especially by obtaining more accurate Yarkovsky calibrations, this can be the beginning of a real asteroid belt chronology. The large compilations of family ages, such as Nesvorný et al. (2005) and Brož et al. (2013) are very useful to confirm that our results are reasonable. When available, the uncertainties reported in these compilations are generally larger; often only upper/lower bounds are given. However, the literature as analyzed in Section 4.2 shows that often results obtained with different methods, even by the same authors, can be discordant. Thus the comparison of ages for different families should not be done with the ages listed in a compilation, but only from a list of ages computed with a single consistent method, including a single consistent calibration scheme, as in this paper.

In the previous paper Milani et al. (2014) we had introduced the distinction between dynamical and collisional families; out of the 5 dynamical families we analyzed as examples, we found 3 cases in which a dynamical family corresponds to at least 2 collisional ones. In this paper we report on the results of a systematic survey of the largest (by number of members) dynamical families, monitoring whether the 1 to 1 correspondence with collisional families does or does not apply.

We have found two examples, for which we use the definition of *family join*, in which two separate dynamical families together form a single V-shape, with consistent slopes, thus indicating a single collisional event: this applies to families 10955 and 19466, 163 and 5026. Note that this is distinct from a *family merge* which can arise when two families, as a result of adding new members with recently computed proper elements, acquire some members in common (Knežević et al., 2014).

We have also found at least three examples of dynamical families containing multiple collisional families: 4, 15 and 1521. For these we have obtained discordant slopes from the IN and the OUT side of the V-shape, resulting in distinct ages, see Fig. 5. We have found a dubious case, family 3, and there are several other cases already either known or suspected.

Finally, we have found two cases of families containing a conspicuous subfamily, with a sharp number density contrast, such that it is possible to measure the slope of a distinct V-shape for the subfamily, thus the age of the secondary collision: the subfamily 3395 of 847, and 15124 of 569. There are several cases of subfamilies, with a separate collisional age, already reported in the literature, but they are mostly from recent (<10 Myr of age) collisions: we have identified subfamilies with ages of ~100 Myr.

From the above discussion, we think a new paradigm emerges: whenever a family age computation is performed, the question on the minimum number of collisional events capable of generating the observed distribution of members of the family in the classification space has to be analyzed. This needs to take also into account other families in the neighborhood (in the classification space). In our case, the classification space is the 3-dimensional proper elements space because we use dynamical families, but note that the same argument applies also to other classifications made in different spaces, such as the ones containing also physical observations data: separate collisional families may well have the same composition.

[8] See the figure 3827_vshapea.eps in the supplementary material.

[9] Plus one possible, a second age for the family 3 (Juno) with a moderate significance in the slope ratio, see Table 4.

[10] To locate these families in the asteroid belt, the best way is to use the graphic visualizer of asteroid families provided by the AstDyS site at http://hamilton.dm.unipi.it/astdys2/Plot/.

[11] For 847 we have used the IN age and STD, as discussed in Section 3.

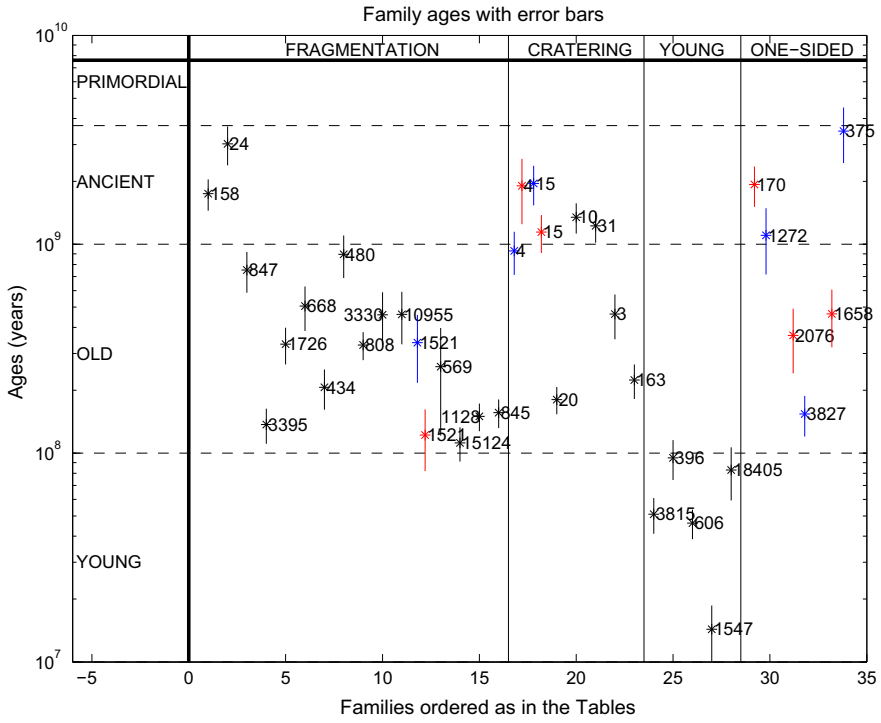

Fig. 5. Family ages and their uncertainties computed in this paper. If two ages of the same family are incompatible, the figure shows both ages; this applies to families 4, 15, 1521. The horizontal dashed lines separate the conventional age groupings, the vertical solid lines separate the family types, for the definitions see in the text.

5.2. Open problems

On other issues we have accumulated data, useful to constrain the asteroid families evolution, but we do not have a full model.

An example is the fact already known that many families have a central gap, in the sense of a bimodal number frequency distribution of members as a function of proper *a*. The interpretation of this gap as a consequence of the interaction between the YORP and the Yarkovsky effect, as proposed in Vokrouhlický et al. (2006b), is plausible and widely accepted, but a model capable of predicting the timescales of this evolution is not available.

We have observed the presence and depth of the gap for all the families having, in our best estimate, <600 Myr.

- Ages between 10 and 100 Myr: the gap does not occur in the youngest 1547 and the one near the upper limit of 100 Myr, that is 396, but occurs in 18405 which has an age similar to 396, and in the two with ages ∼50 Myr, 3815 and 606.
- Ages between 100 and 200 Myr: the gap occurs consistently in families such as 3395, 15124, 1128, 845, and less deep in 20.
- Ages between 200 and 400 Myr: there are three families with gap (434, 808, 163) and two without (1726, 3).
- Ages between 400 and 600 Myr: 10955 has a gap and 668 does not.
- Ages >600 Myr: among the ancient families only 158 and maybe 31 show some small dip in density at the center.

These results do not contradict the interpretation that YORP moves the rotation axes towards the spin up/spin down position, but takes quite some time to achieve a strong bimodality which gradually empties the gap. Over longer time scales, spin axis randomization can reverse the process. However, our set of examples above shows that the time scales for such processes are not uniform, but may substantially change from family to family.

Another open problem results from the fact that several families on the outer edge of the 3/1 resonance gap appear to have a boundary close to, but not at the Kirkwood gap. This happens to the IN side of families 480 and 15; there are also families 170 and 1658 which are one-sided because of the missing IN side, with the family not touching the gap. This might require a dedicated study to find a plausible explanation.

5.3. Family ages left to be computed

Of the dynamical families in the current classification, there are 11 with >300 members for which we have not yet computed a satisfactory age. The motivations are as follows:

- There are five complex families: 135, known to have at least two collisional families, with incompatible physical properties, difficult to disentangle; see e.g., Milani et al. (2014, Fig. 10); 221, complex both for dynamical evolution (Vokrouhlický et al., 2006c) and suspect of multiple collisions; 145, which appears to have at least 2 ages; 25, corresponding to a stable region surrounded by secular resonances, could have many collisional families; 179, a cratering family which is difficult to be interpreted.
- There are another four families strongly affected in their shape in proper element space by resonances: 5, 110, 283 with secular resonances, and 1911 inside the 3/2 resonance.
- Two others: 490, well known to be of recent age (Nesvorný et al., 2003; Tsiganis et al., 2007); 1040, at large proper $\sin I$ and also quite large e; both are strongly affected by 3-body resonances.

We are convinced that for many of these it will be possible to estimate the age, but this might require ad hoc methods, different from case to case. In this paper we have included all the ages which we have up to now been able to estimate by a uniform method.

Other families with marginal number of members for the V-shape fit (between 100 and 300 in the current classification)

could become suitable as new proper elements are computed and the classification is automatically updated, especially in the zones where the number density is low, such as the high I region, and the Cybele region, beyond the 2/1 resonance.

Acknowledgments

The authors have been supported for this research by: ITN Marie Curie "STARDUST – the Asteroid and Space Debris Network" (FP7-PEOPLE-2012-ITN, Project Number 317185) (A.M. and Z.K), the Department of Mathematics of the University of Pisa (A.M. and F.S.), SpaceDyS srl, Cascina, Italy (F.S.), and the Ministry of Education, Science and Technological Development of Serbia, under the project 176011 (Z.K.).

The authors would also like to thank Melissa Dykhuis and Marco Delbò for their helpful comments.

References

Bottke, W.F., Vokrouhlický, D., Nesvorný, D., 2007. An asteroid breakup 160 Myr ago as the probable source of the K/T impactor. Nature 449 (September), 48–53.
Bottke, W.F. et al., 2015. In search of the source of asteroid (101955) Bennu: Applications of the stochastic YORP model. Icarus 245 (January), 191–217.
Brož, M. et al., 2013. Constraining the cometary flux through the asteroid belt during the late heavy bombardment. Astron. Astrophys. 551 (March), A117.
Carpino, M., Milani, A., Chesley, S.R., 2003. Error statistics of asteroid optical astrometric observations. Icarus 166 (December), 248–270.
Carruba, V., 2010. The stable archipelago in the region of the Pallas and Hansa dynamical families. MNRAS 408 (October), 580–600.
Carry, B., 2012. Density of asteroids. Planet. Space Sci. 73, 98–118.
Chapman, C.R. et al., 1996. Cratering on Ida. Icarus 120 (March), 77–86.
Chesley, S.R. et al., 2014. Orbit and bulk density of the OSIRIS-REx target Asteroid (101955) Bennu. Icarus 235 (June), 5–22.
Delisle, J.-B., Laskar, J., 2012. Chaotic diffusion of the Vesta family induced by close encounters with massive asteroids. Astron. Astrophys. 540 (April), A118.
Farinella, P., Davis, D.R., Marzari, F., 1996. Asteroid families, old and young. In: Rettig, T., Hahn, J.M. (Eds.), Completing the Inventory of the Solar System, Astronomical Society of the Pacific Conference Series, vol. 107, pp. 45–55.
Greenberg, R. et al., 1996. Collisional and dynamical history of Ida. Icarus 120 (March), 106–118.
Knežević, Z. et al., 2014. Automated classification of asteroids into families at work. In: Knežević, Z., Lemaitre, A. (Eds.), Complex Planetary Systems, Proceedings of the IAU Symposia. Cambridge Univ. Press, pp. 130–133.
Mainzer, A. et al., 2011. NEOWISE observations of Near-Earth objects: Preliminary results. Astrophys. J. 743 (December), 156.
Marchi, S. et al., 2012. The violent collisional history of Asteroid 4 Vesta. Science 336 (May), 690–694.
Marzari, F., Davis, D., Vanzani, V., 1995. Collisional evolution of asteroid families. Icarus 113 (January), 168–187.
Masiero, J.R. et al., 2011. Main belt asteroids with WISE/NEOWISE.I. Preliminary albedos and diameters. Astrophys. J. 741 (November), 68.
Milani, A. et al., 2010. Dynamics of the Hungaria asteroids. Icarus 207 (June), 769–794.
Milani, A. et al., 2014. Asteroid families classification: Exploiting very large datasets. Icarus 239, 46–73.
Nesvorný, D. et al., 2003. Recent origin of the Solar System dust bands. Astrophys. J. 591 (July), 486–497.
Nesvorný, D. et al., 2005. Evidence for asteroid space weathering from the Sloan Digital Sky Survey. Icarus 173 (January), 132–152.
Nesvorný, D. et al., 2009. Asteroidal source of L chondrite meteorites. Icarus 200 (April), 698–701.
O'Brien, D.P. et al., 2014. Constraining the cratering chronology of Vesta. Planet. Space Sci. 103 (November), 131–142.
Pravec, P. et al., 2012. Absolute magnitudes of asteroids and a revision of asteroid albedo estimates from WISE thermal observations. Icarus 221 (September), 365–387.
Shepard, M.K. et al., 2008. Radar observations of E-class Asteroids 44 Nysa and 434 Hungaria. Icarus 195 (May), 220–225.
Tsiganis, K., Knežević, Z., Varvoglis, H., 2007. Reconstructing the orbital history of the Veritas family. Icarus 186 (February), 484–497.
Vokrouhlický, D. et al., 2006a. The peculiar case of the Agnia asteroid family. Icarus 183 (August), 349–361.
Vokrouhlický, D. et al., 2006b. Yarkovsky/YORP chronology of asteroid families. Icarus 182 (May), 118–142.
Vokrouhlický, D. et al., 2006c. Yarkovsky footprints in the Eos family. Icarus 182 (May), 92–117.
Vokrouhlický, D. et al., 2010. Collisionally born family about 87 Sylvia. Astron. J. 139 (June), 2148–2158.
Vokrouhlický, D., Milani, A., Chesley, S.R., 2000. Yarkovsky effect on small Near-Earth asteroids: Mathematical formulation and examples. Icarus 148, 118–138.
Warner, B.D. et al., 2009. Analysis of the Hungaria asteroid population. Icarus 204 (November), 172–182.
Wright, E.L. et al., 2010. The Wide-field Infrared Survey Explorer (WISE): Mission description and initial on-orbit performance. Astron. J. 140 (December), 1868–1881.
Zappalá, V. et al., 1990. Asteroid families. I – Identification by hierarchical clustering and reliability assessment. Astron. J. 100, 2030–2046.